Revue des Composites et des Matériaux Avancés-Journal of Composite and Advanced Materials
Vol. 36, No. 1, February, 2026, pp. 59-67
Journal homepage: http://iieta.org/journals/rcma

Metal Oxide-Modulated PEO/PANI Nanocomposites for High-Performance Ammonia Sensing: The Critical Role of NiO Heterojunctions

Rusul K. Jasim*, Mohammed H. Shinen, Saba A. Obaid

Department of Physics, College of Science, University of Babylon, Babil 51001, Iraq

Corresponding Author Email: rusulkadhom7@gmail.com

https://doi.org/10.18280/rcma.360106

Received: 1 October 2025
Revised: 28 December 2025
Accepted: 15 February 2026
Available online: 28 February 2026

Keywords:
PEO/PANI nanocomposites, ammonia gas sensor, metal oxide doping, NiO heterojunction, charge transport mechanism

ABSTRACT

Conducting polymer-based nanocomposites offer a promising avenue for cost-effective gas sensing, yet optimizing their sensitivity and stability remains a challenge. This work investigates the ammonia (NH_3) sensing performance of poly(ethylene oxide) (PEO)/polyaniline (PANI) composites incorporated with WO_3, Cr_2O_3, and NiO nanoparticles. Fabricated via solution casting, the nanocomposites were characterized by X-ray diffraction (XRD) and field-emission scanning electron microscopy (FESEM), followed by DC conductivity and gas sensing measurements at room temperature, 100°C, and 200°C. Structural analysis confirms a semi-crystalline morphology with successful nanoparticle embedding. Notably, the NiO-doped sample (NC3) exhibits enhanced surface roughness and porosity, facilitating gas diffusion. Electrical measurements reveal a thermally activated hopping mechanism, where NC3 demonstrates the highest conductivity due to strong electronic coupling between NiO and PANI. At 100°C, NC3 achieves a maximum sensitivity of 36.71% toward NH_3, with response and recovery times of 18.36 s and 18.63 s, respectively, outperforming counterparts doped with WO_3 or Cr_2O_3. This superior performance is attributed to the p-type semiconducting nature of NiO, its catalytic activity, and the formation of polymer-oxide heterojunctions that accelerate charge transfer. These findings suggest that strategic metal oxide selection effectively tailors the structural and electronic properties of polymer composites, providing a viable strategy for designing low-cost, stable ammonia sensors.

1. INTRODUCTION

Ammonia (NH_3) is a poisonous and corrosive gas widely used in industry, agriculture, and medicine. Even at low concentrations, it can cause severe irritation to humans and harm the environment. Hence, the NH_3 measurement is urgent to safeguard safety and the environment [1]. The conducting polymer, in particular polyaniline (PANI), has been widely studied by several workers because of its ability and variability in electrical conductivity and strong response to reducing gases, NH_3, which causes measurable variation of electrical resistance [2]. Performance indicators for gas sensors include sensitivity, response/recovery times, and long-term stability, among others [3]. Nanoscale phases with high interfacial areas into polymer matrices have been reported to enhance the physicochemical properties of nanocomposite systems when compared to traditional micro-composite materials [4, 5]. Nano-oxides such as tungsten trioxide (WO_3), chromium(III) oxide (Cr_2O_3), nickel oxide (NiO), etc., are used extensively in gas sensors due to their catalytic activity and chemical inertness. WO_3 is a n-type semiconducting oxide that has been recognized for its NH_3-sensitivity [6, 7]. PEO/PANI blends offer mechanical flexibility and tunable conductivity, which are desirable for sensing applications [8-13]. Cr_2O_3 adds chemical hardness and stability [14]. In addition, NiO–a low-cost p-type oxide–shows vigorous catalytic activity and enhanced charge-transfer in sensing devices [15, 16].

2. EXPERIMENTAL

Polyethene oxide (PEO) is a white, crystalline, granular polymer with the chemical structure $H–(OCH_2CH_2)_n–OH$ and a high molecular weight of 3,000,000 g/mol. It is characterised by good solubility, film-forming ability, and semi-crystalline behaviour. Polyaniline (PANI) has a particle size of roughly 20 nm. Its general formula is $(C_6H_7N)_n$, and its colour varies with oxidation state, usually appearing dark green or black in

powder form. Tungsten trioxide (WO_3) is a yellow nanopowder with a particle size of about 50 nm, 99.9% purity, and a molecular weight of 231.84 g/mol. It typically exhibits a monoclinic crystal structure at room temperature and a melting point of 1473°C. WO_3. Chromium(III) oxide (Cr_2O_3), a dark green nano powder with 99% purity and ~ 50 nm particle size. Nickel oxide (NiO) is a black nano powder with 99.5% purity and an average particle size of 50 nm. The mass of each component employed for the fabrication of PEO/PANI nanocomposite samples doped with WO_3, Cr_2O_3, and NiO is shown in Table 1.

Table 1. Composition and specifications of materials used for the synthesis of PEO/PANI blend and nanocomposites.

Sample	Mass (g)	Distilled Water (mL)	Molecular Weight (g/mol)	Company
PEO	1.5	450	3,000,000	Panichem Co., Ltd. South Korea
PANI	1	100	150,000	Cheng Du Micxy Chemical Co., Ltd., China
WO_3	0.05	50	231.84	Hongwu International Group Ltd. China
Cr_2O_3	0.05	50	151.99	Telligent Materials Pvt.Ltd, India
NiO	0.05	50	74.69	Sky Spring Nanomaterials, Inc. The United States

Note: Tungsten trioxide (WO_3); Chromium(III) oxide (Cr_2O_3); Nickel oxide (NiO); Polyethene oxide (PEO); Polyaniline (PANI).

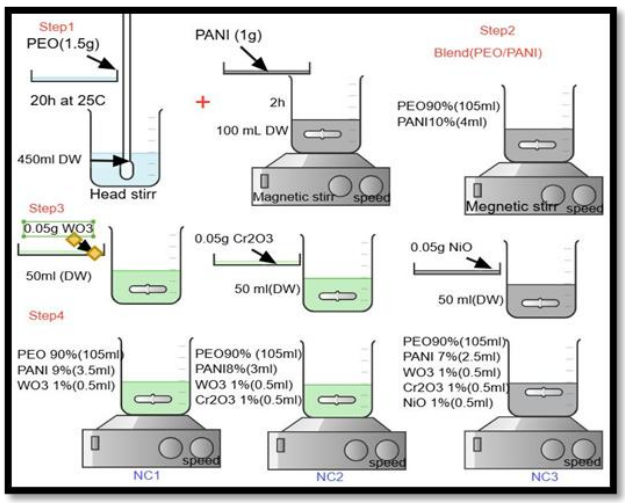

Figure 1. Schematic illustration of the solution-casting fabrication process for PEO/PANI blend and metal oxide-doped nanocomposite films

Table 2. Concentration of PEO/PANI blend and Nanocomposites

Polymer	PANI	WO_3	Cr_2O_3	NiO
PEO 90%	10	-	-	-
PEO 90%	9	1	-	-
PEO 90%	8	1	1	-
PEO 90%	7	1	1	1

Note: Polyaniline (PANI); Tungsten trioxide (WO_3); Chromium(III) oxide (Cr_2O_3); Nickel oxide (NiO); Polyethene oxide (PEO).

2.2 Film formation

The PEO/PANI composite was fabricated by slowly dissolving 0.5 g of PEO in 150 mL of distilled water (DW) under an overhead mechanical stirrer at a regular stirring speed of 500 rpm for 4 h at ~ 25°C. Separately, 1.0 g of polyaniline (PANI) was dispersed in 100 mL DW and magnetically stirred for 2 h to form a PANI dispersion. The two solutions were then mixed at a 90:10 (PEO: PANI) weight ratio and stirred for an additional 2 h under mechanical stirring to yield a homogeneous polymer matrix. The metal oxide–doped nanocomposites were prepared by dispersing 0.05 g of the oxides (WO_3, Cr_2O_3, or NiO) each in 50 mL DW individually and magnetically stirred for 1.5 h with the addition of 2 mL from each suspension to the PEO/PANI blend while stirring continuously to ensure uniform dispersion of the nanoparticles. The resultant mixtures are named as WO_3 Doped Composite, NC1; Cr_2O_3 Doped Composite, NC2, and NiO Doped Composite, NC3, respectively. When the mixture was thoroughly homogenized, each mix was spread on a glass substrate and allowed to dry undisturbed at ~ 25°C for 10 days. The slow evaporation allowed the formation of regular, mechanically stable thin films with enhanced polymer–oxide interaction. The detailed preparation process is shown in Figure 1. The compositions are presented in Table 2.

3. RESULTS AND DISCUSSION

3.1 Structural and morphological properties

The X-ray diffraction (XRD) pattern of the pure PEO/PANI blend (sample B) confirms its semi-crystalline character, a common property of polymeric systems where chain entanglement and structural disorder inhibit long-range orderIts semi-crystalline character, a common property of polymeric systems, is where chain entanglement and structural disorder inhibit long-range order. After incorporation of the MO NPs, nanocomposites (NC1, NC2, and NC3) reveal a few sharp diffraction peaks, reflecting that the crystalline phase of oxide is successfully incorporated into the polymer matrix [17].

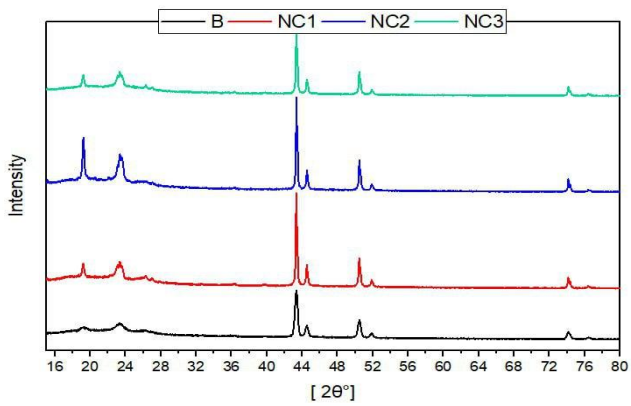

Figure 2. X-ray diffraction (XRD) patterns of pure PEO/PANI blend and nanocomposites doped with WO_3, Cr_2O_3, and NiO

NC2 exhibits reflections corresponding to JCPDS 38-1479 from Cr_2O_3, consistent with the reported data of Cr_2O_3 [18]. The cubic NiO-doped composite (NC3) shows strong peaks attributable to cubic NiO (JCPDS 47-1049), suggesting that the structural stability of NiO nanoparticles was maintained through dispersing into a polymer matrix [19]. A gradual increase in the intensity of the peak maximum and partial sharpening of the PEO/PANI peaks from NC1 to NC3 is indicative of improved structural ordering, probably caused by a nucleation effect on polymer molecules exerted by NPs, favouring local alignment of polymer chains. Similar enhancement of crystallinity effects in polymer–oxide composites has been described in previous work. Crystallinity is highest in sample NC3, which suggests strong polymer–oxide affinities; no impurity phases are found in any of the films. The general XRD characterization results shown in Figure 2 show that the presence of oxide drastically changes the structural morphology of the PEO/PANI matrix, which is thought to tailor its electrical and gas-sensing behavior.

The field-emission scanning electron microscopy (FESEM) images of (B, NC1, NC2, and NC3) reveal the definite morphological changes due to metal oxide doping. The as-prepared blend (B) has a smooth and nonporous surface, which is usually observed for a polymer matrix without inorganic filler [2], consistent with earlier results of PEO-based systems [20]. When WO_3 is added to the particles, it gives rise to small granular elements that cover the surface of sample NC1, resulting in a moderate increase in roughness. The Cr_2O_3-containing NC2 composite exhibits more noticeable texturing, finer grains, and higher surface irregularity of the oxide phase, indicating further dispersion and better polymer–oxide interfacial interaction. The morphology change upon the addition of oxides has been well reported in polymer/metal-oxide hybrids [21].

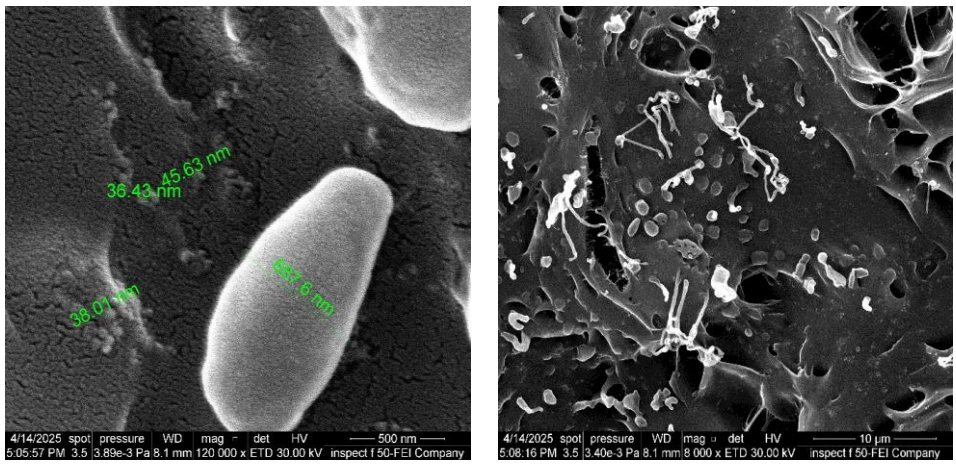

B

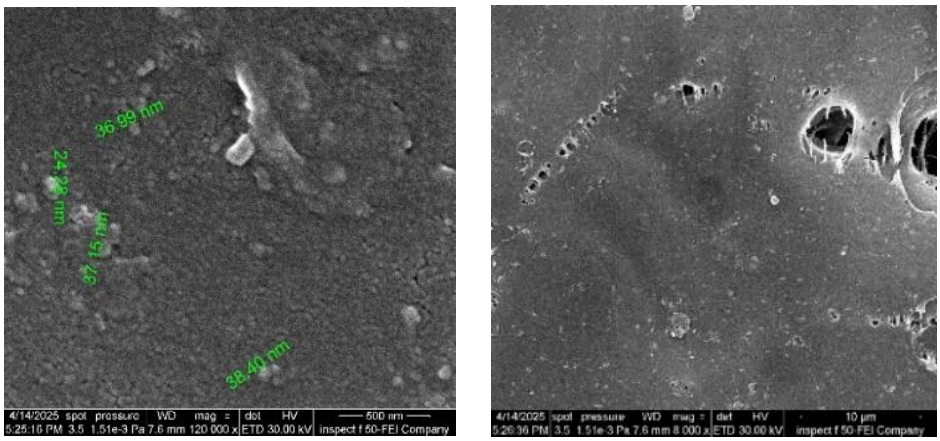

NC1

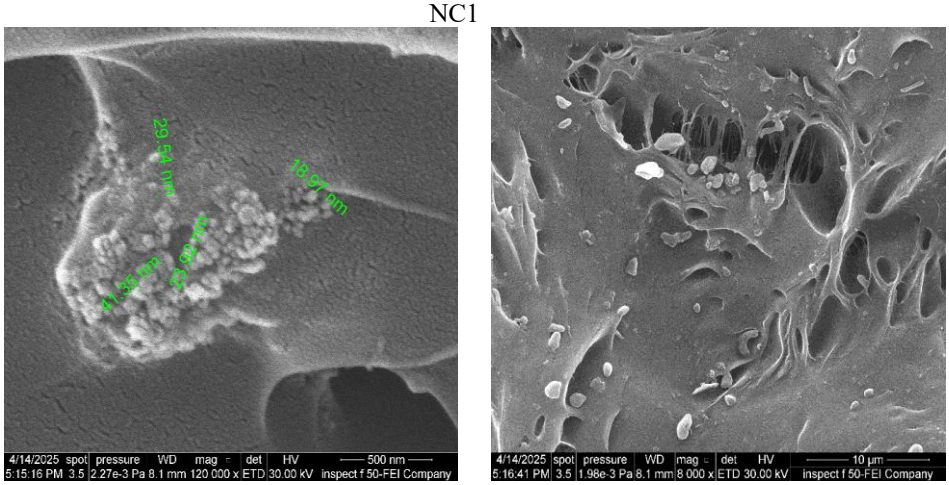

NC2

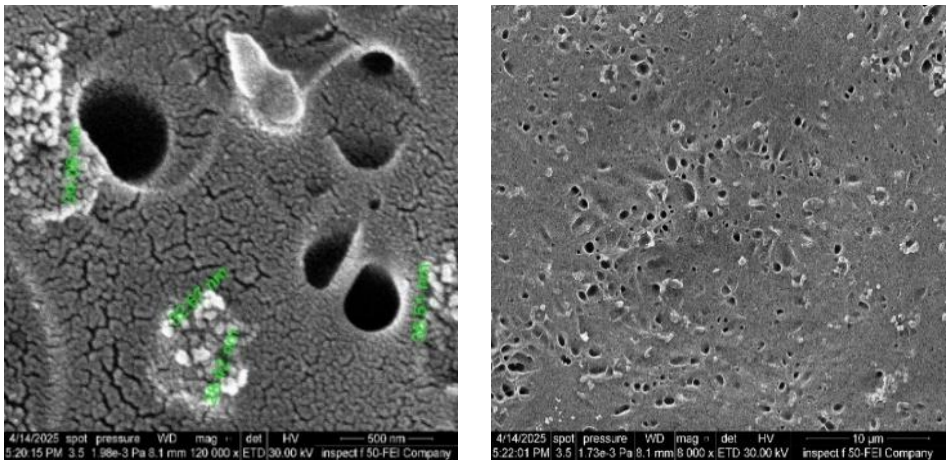
NC3

Figure 3. The Field-emission scanning electron microscopy (FESEM) analysis shows nanoscale and microscale surface structures of (B, NC1, NC2, and NC3)

The NC3 film doped with NiO shows the most pronounced morphological change. The surface becomes very porous with interconnected grains and open channels, suggesting a significant enhancement of the active surface area. Shape-induced enhancements in functional properties—especially when the presence of nanostructured fillers may generate roughness and porosity—have been analogously described also for polymer nanoparticle systems [22].

The structural variations are in excellent agreement with the sensing properties: enhanced porosity and grain connectivity of NC3 lead to a fast NH_3 adsorption–desorption, which accounts for why NC3 exhibits greatly improved sensitivity and shorter response–recovery times than those of B, NC1, and NC2. These findings indicate that the particles possess stable and uniform morphology (Figure 3).

3.2 Electrical properties

3.2.1 DC electrical conductivity

DC conductivity of all samples (B, NC1, NC2, and NC3) increases with temperature, indicating a thermally activated hopping mechanism typical of polymer electrolytes and conducting polymer systems [23]. At low temperatures, restricted chain mobility limits charge motion, while increasing temperature enhances segmental dynamics and enables more efficient carrier hopping. The pure blend (B) shows the lowest conductivity due to the absence of inorganic fillers and its partially crystalline structure, which introduces higher transport barriers. The incorporation of WO_3 in NC1 and Cr_2O_3 in NC2 improves conductivity by providing additional charge pathways and increasing interfacial polarization within the polymer matrix. Such oxide-induced enhancement of conduction has been widely reported in polymer/metal-oxide nanocomposites [24].

NC3 (NiO/PEO/PANI) exhibits the highest conductivity among all samples. This improvement is attributed to the semiconducting nature of NiO, its strong electronic interaction with PANI, and the formation of interconnected porous pathways observed in FESEM. These structural features facilitate polaron/bipolaron transport and lower the activation energy for charge motion, consistent with previous studies on NiO-containing conductive polymer systems [25]. The overall conductivity trend B < NC1 < NC2 < NC3 aligns directly with the increasing structural ordering and porosity, as shown in Figure 4.

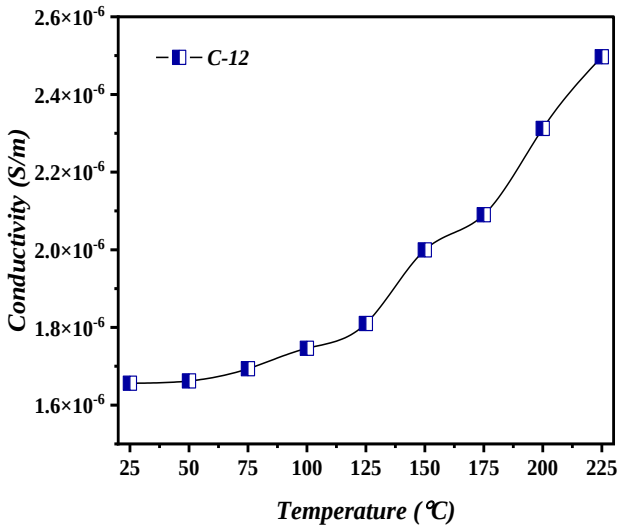

B

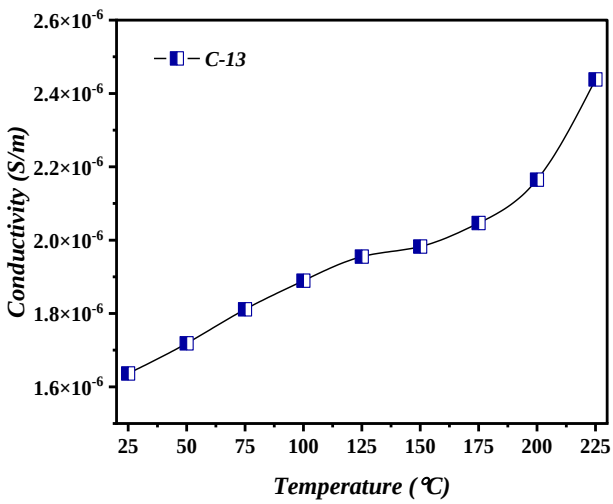

NC1

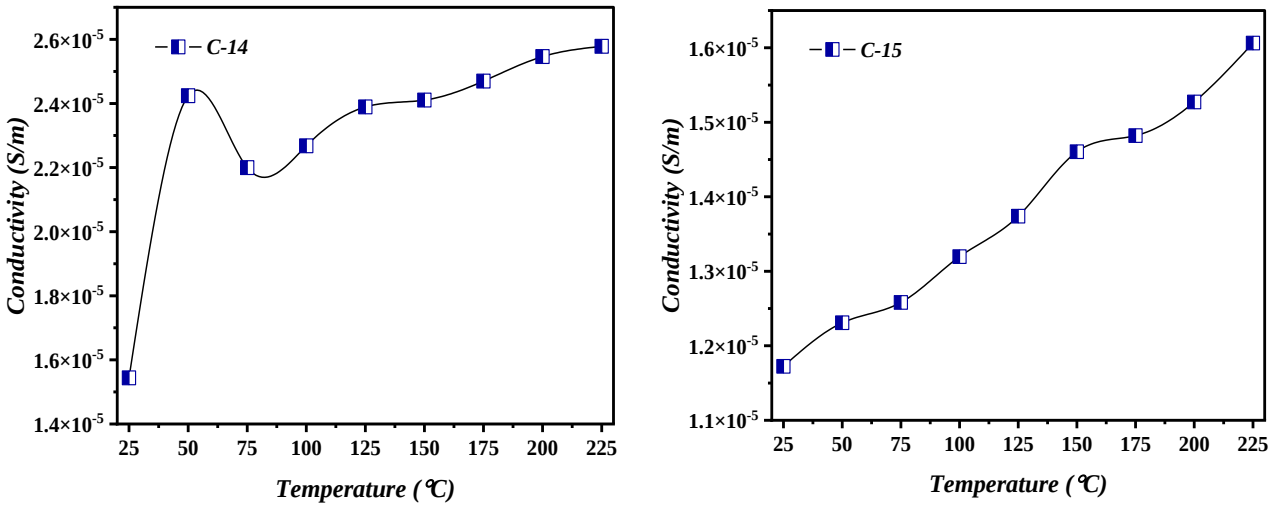

NC2 NC3

Figure 4. The electrical conductivity was evaluated for (B, NC1, NC2, and NC3)

3.3 Gas sensing of NH_3

The sensing performance of blend (B) and nanocomposite-based sensors (NC1, NC2, NC3) towards ammonia gas (NH_3) was investigated at room temperature and at 100℃, as well as 200℃. As seen in Figures (5-7), all the sensors displayed a reversible change in resistance upon exposure to NH_3 characteristic of p-type conductive polymers like PANI. The NH_3 molecules are found to be electron donors, which reduces the hole concentration and results in resistance fall [26, 27]. The increase in operating temperature the gas–solid interaction, and is also for faster adsorption–desorption kinetics and better stability of the response cycles. This behavior is also apparent at 100℃, for which the resistance transitions are sharper in all cases and the speed of response time/recovery time is diminished relative to ambient temperature, consistent with thermally activated sensing shown previously in polymer–oxide hybrids [28, 29].

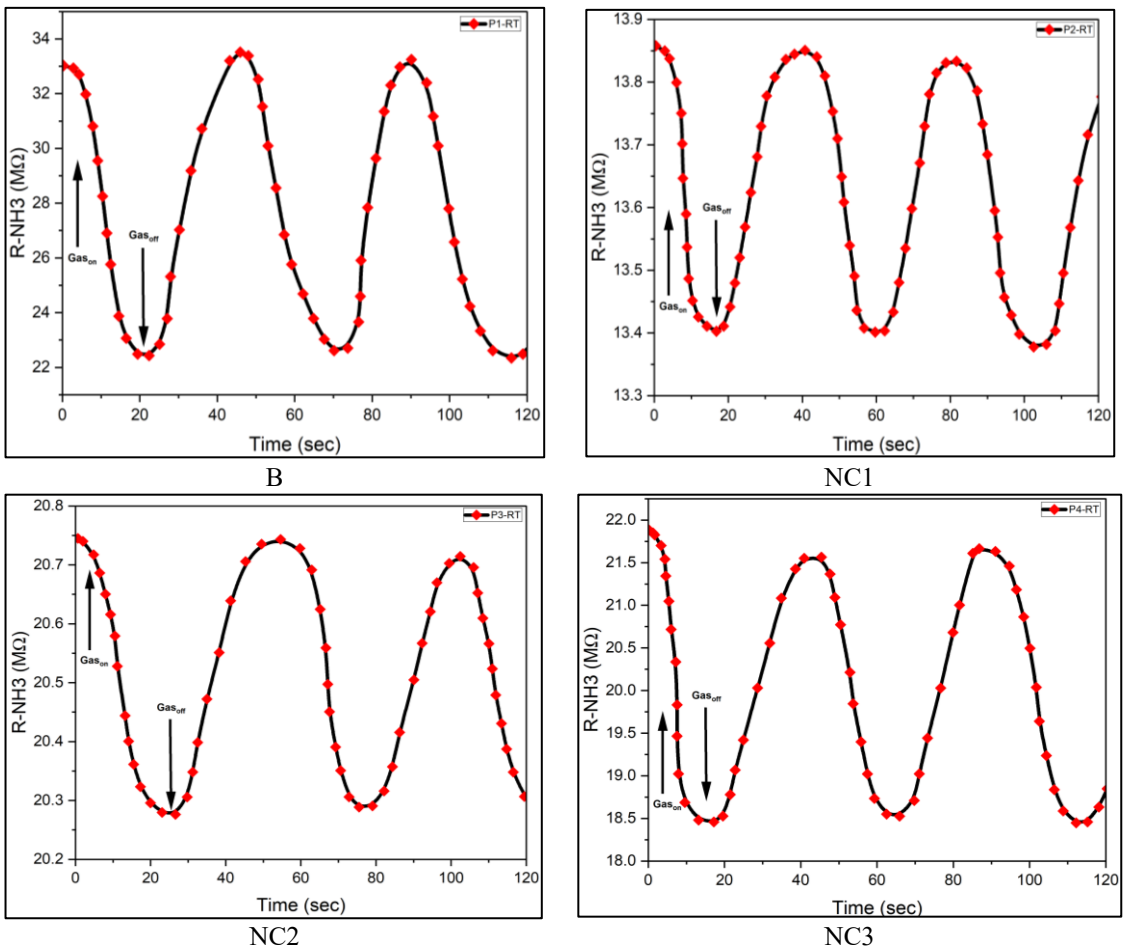

B NC1

NC2 NC3

Figure 5. Resistance versus time changes in (B, NC1, NC2, and NC3) exposed to NH_3 gas at RT

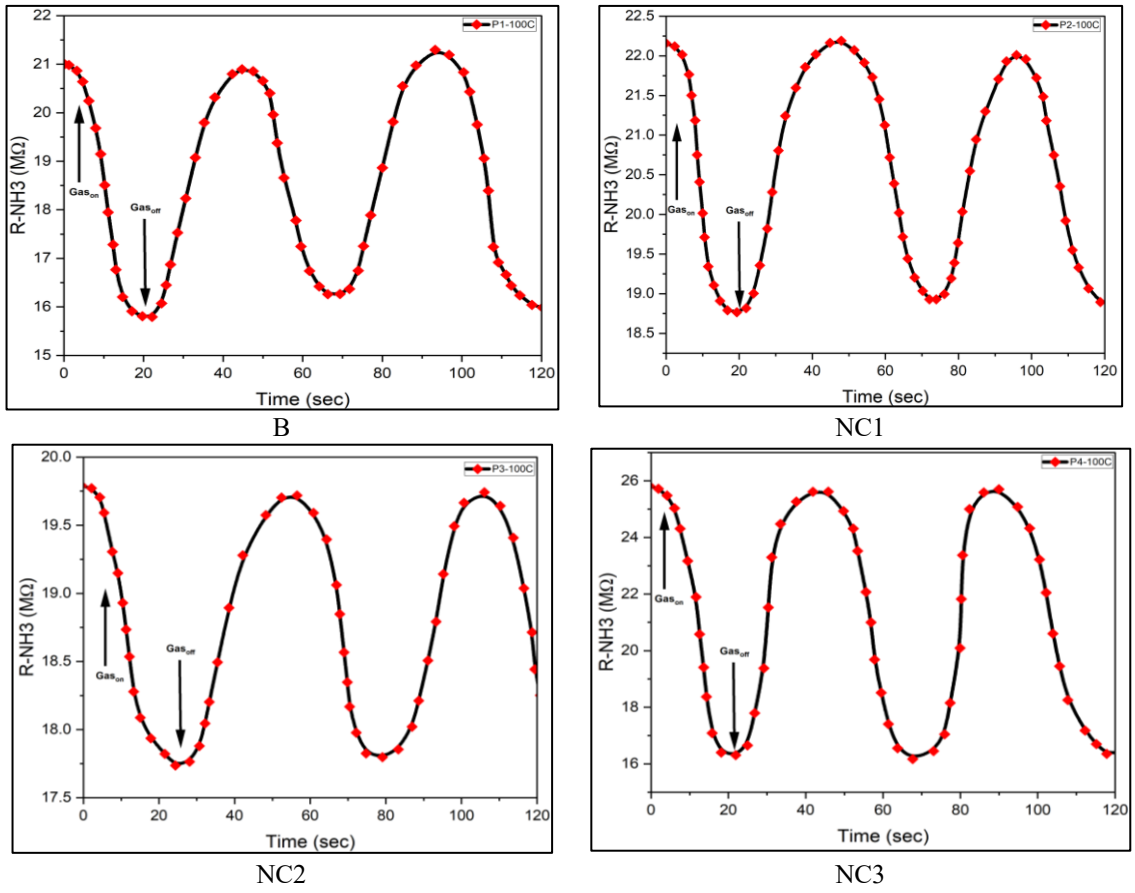

Figure 6. Resistance versus time changes in (B, NC1, NC2, and NC3) exposed to NH_3 gas at 100°C

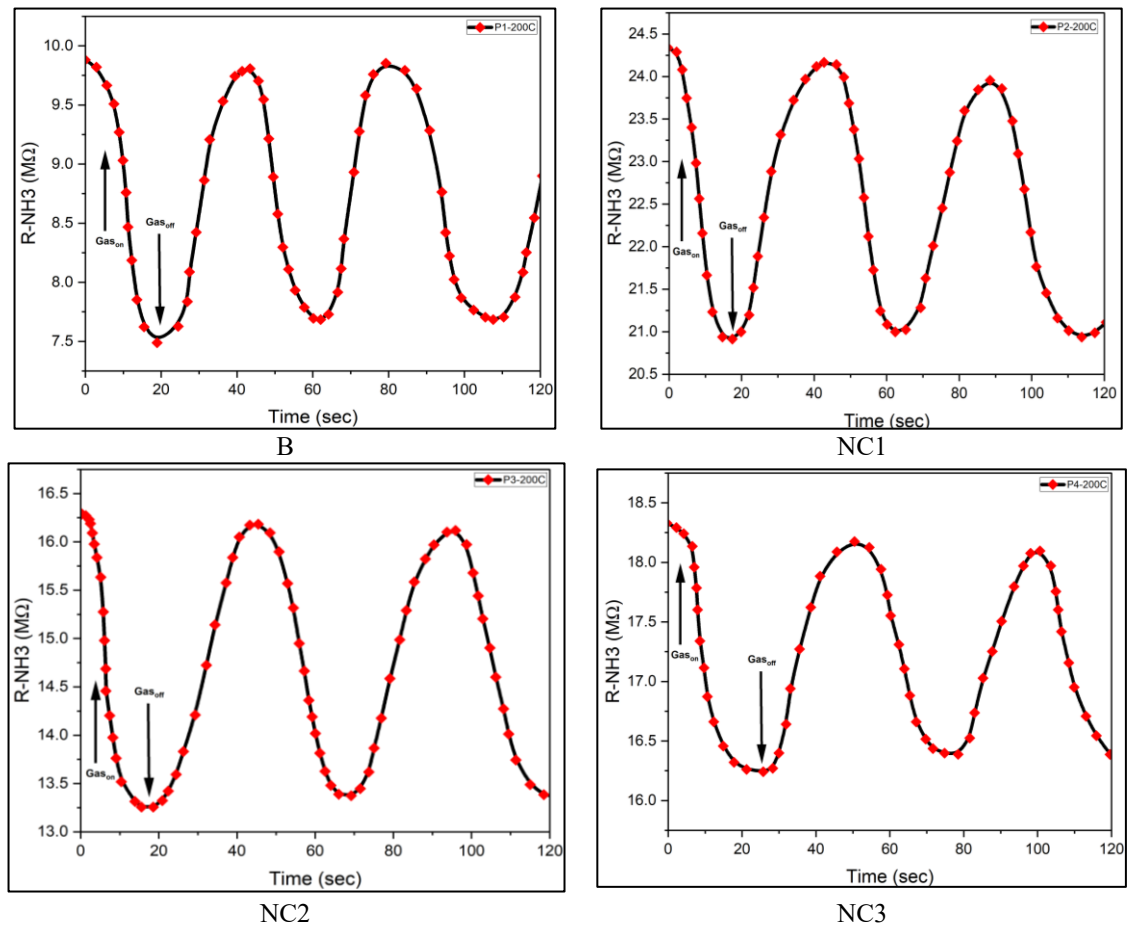

Figure 7. Resistance versus time changes in (B, NC1, NC2, and NC3) exposed to NH_3 gas at 200°C

Table 3 shows that Al- and metal oxide-doping had obvious effects on the sensitivity, response time, and recovery time of NH_3 detection. The sensing of the pure blend is further improved for NC1 (WO_3/PEO/PANI) and NC2 (Cr_2O_3/PEO/PANI) because of the catalytic properties of the metal oxide and a larger number of adsorption sites. WO_3 and Cr_2O_3 also promote charge transfer across the polymer–oxide interface, leading to sufficient modulation of resistance upon exposure to NH_3 [30]. At 100°C, NC3 exhibits the highest sensitivity (36.71%). However, its response time (18.36 s) is shorter than that of NC2 (20.43 s) but slightly longer than that of B (16.56 s) and NC1 (15.03 s), indicating a competitive rather than superior response performance. The improved response of NC3 can be attributed to (i) p-type nature of NiO semiconducting, (ii) the strong electronic coupling between PANI and NiO, and (iii) enhanced charge-transfer pathways, as well as (iv) its highly porous morphology observed from FESEM, which promote a quicker diffusion/adsorption kinetics of NH_3 molecules [31-33] These synergistic effects decrease the activation barrier for charging modulation and lead to fast recovery and sensitivity/responsivity. Even at 200°C, each of the samples shows periodic and reversible resistance change, suggesting good thermal stability of sensing films [34]. On the whole, the performance sequence < NC2 < NC1 < B < NC3 reflects well the crystalline ordering, electrical conductivity, and surface reactivity of the oxide, evidencing that the selection of oxides is an effective route to optimizing NH_3 sensing performance.

Table 3. The relation between temperature and sensitivity, response time, and recovery time

Sample	T °C	Sensetivity-NH_3 %	Response Time sec	Recovery Time sec
B	RT	32.21	15.39	22.14
	100	24.88	16.56	21.42
	200	23.71	13.68	18.63
NC1	RT	2.89	12.6	20.79
	100	14.54	15.03	24.12
	200	13.63	14.49	21.06
NC2	RT	2.41	17.46	29.7
	100	9.69	20.43	28.08
	200	18.51	14.4	24.03
NC3	RT	15.20	13.05	24.39
	100	36.71	18.36	18.63
	200	12.08	21.33	20.88

4. CONCLUSIONS

In this study, PEO/PANI nanocomposites doped with WO_3, Cr_2O_3, and NiO have been fabricated and studied for their structural, electrical, and ammonia-sensing behavior. XRD showed that the semi-crystalline feature of the polymer blend was not altered by the incorporation of MOs, except for a slight modification in the lattice, suggesting improved structural ordering. FESEM image showed that the introduction of oxide was inclined to increase surface roughness as well as porosity, especially in the NiO-doped sample, and sooner or later resulted in an easier accessible adsorption site for gas molecules. The DC conductivity for all the samples was found to be increased with a rise in temperature, obeying a thermally activated hopping mechanism. Doping with metal oxides enhanced the charge transfer considerably by creating extra conduction channels; NC3 had gained a highest conductivity value because of remarkably strengthened interface interaction between NiO and PANI. Gas-sensing tests revealed the dependence of sensor performance on operation temperature and, 100°C was found to be the best temperature for detecting NH_3. For all samples, NC3 exhibited better sensitivity (36.7%) and short response/recovery times which may be ascribed to its porous structure, fast charge-transfer process and intrinsic catalytic activity of NiO. In summary, the results confirm that oxide choice plays a significant role in controlling the structural, electrical and sensing performance of PEO/PANI composites. The excellent activity of NC3 indicates that NiO-doped conducting polymer nanocomposites are promising for high-efficiency, thermal-stable and low-cost ammonia gas sensors

REFERENCES

[1] Timmer, B., Olthuis, W., and van den Berg, A. (2005). Ammonia sensors and their applications—A review. Sensors and Actuators B: Chemical, 107(2): 666-677. https://doi.org/10.1016/j.snb.2004.11.054

[2] Wen, J., Wang, S., Feng, J., Ma, J., Zhang, H., Wu, P., Li, G., Wu, Z., Meng, F., Li, L., Tian, Y. (2024). Recent progress in polyaniline-based chemiresistive flexible gas sensors: Design, nanostructures, and composite materials. Journal of Materials Chemistry A. https://doi.org/10.1039/D3TA07687C

[3] Schütze, A., Baur, T., Leidinger, M., Reimringer, W., Jung, R., Conrad, T., Sauerwald, T. (2017). Highly sensitive and selective VOC sensor systems based on semiconductor gas sensors: how to? Environments, 4(1): 20. https://doi.org/10.3390/environments4010020

[4] Shameem, M.M., Sasikanth, S.M., Annamalai, R., Raman, R.G. (2021). A brief review on polymer nanocomposites and its applications. Materials Today: Proceedings,45:2536-2539. https://doi.org/10.1016/j.matpr.2020.11.254

[5] Al-Bayati, A.A., Ali, H.F. (2025). Synthesis, structural, and optical characterization of ZnO/SnO_2 nanocomposites thin films prepared by spin coating and pulse laser deposition. Iraqi Journal of Physics, 23(1): 68-77. https://doi.org/10.30723/ijp.v23i1.1334

[6] Hu, Q., Wang, Z., Chang, J., Wan, P., Huang, J., Feng, L. (2021). Design and preparation of hollow NiO sphere-polyaniline composite for NH3 gas sensing at room temperature. Sensors and Actuators B: Chemical, 344: 130179. https://doi.org/10.1016/j.snb.2021.130179

[7] Murata, K., Izuchi, S., Yoshihisa, Y. (2000). An overview of the research and development of solid polymer electrolyte batteries. Electrochimica acta, 45(8-9): 1501-1508. https://doi.org/10.1016/S0013-4686(99)00365-5

[8] Alsulami, Q.A., Rajeh, A. (2022). Structural, thermal, optical characterizations of polyaniline/polymethyl methacrylate composite doped by titanium dioxide nanoparticles as an application in optoelectronic devices. Optical Materials, 123: 111820. https://doi.org/10.1016/j.optmat.2021.111820

[9] Aziz, S.B., Abdullah, O.G., Hussein, A.M., Abdulwahid, R.T., et al. (2017). Optical properties of pure and doped PVA: PEO based solid polymer blend electrolytes: two methods for band gap study. Journal of Materials Science: Materials in Electronics, 28(10): 7473-7479. https://doi.org/10.1007/s10854-017-6437-1

[10] Pradeepa, P., Sowmya, G., Kalaiselvimary, J., Prabhu, M.R. (2016). Optimization of hybrid polymer electrolytes with the effect of lithium salt concentration in PEO/PVdF-HFP blends. Materials Science and Engineering: B, 205: 6-17. https://doi.org/10.1016/j.mseb.2015.11.009

[11] Lapienis, G. (2009). Star-shaped polymers having PEO arms. Progress in Polymer Science, 34(9): 852-892. https://doi.org/10.1016/j.progpolymsci.2009.04.006

[12] Mousavi, S., Kang, K., Park, J., Park, I. (2016). A room temperature hydrogen sulfide gas sensor based on electrospun polyaniline–polyethylene oxide nanofibers directly written on flexible substrates. RSC Advances, 6(106): 104131-104138. https://doi.org/10.1039/C6RA20710C

[13] El-Naggar, A.M., Heiba, Z.K., Kamal, A.M., Mohamed, M.B., Altowairqi, Y. (2024). Tuning the structural, optical and dielectric features of PMMA/PEO/PANi blend using nano $MnFe_2O_4$. Optical Materials, 154: 115705. https://doi.org/10.1016/j.optmat.2024.115705

[14] Zhou, P., Tsang, J.H., Blackman, C., Shen, Y., et al. (2024). A novel mechanism based on oxygen vacancies to describe isobutylene and ammonia sensing of p-Type Cr_2O_3 and Ti-Doped Cr_2O_3 Thin Films. Chemosensors, 12(10): 218. https://doi.org/10.3390/chemosensors12100218

[15] Kumar, P., Aslam, M., Ali, S., Hamdy, K., Ahmad, K., Danishuddin. (2025). Progress in NiO based materials for electrochemical sensing applications. Biosensors, 15(10): 678. https://doi.org/10.3390/bios15100678

[16] Shoair, A.G.F., Shanab, M.M., El-Ghamaz, N.A., Abou-Krisha, M.M., Kenawy, S.H., Yousef, T.A. (2023). Green catalytic conversion of some benzylic alcohols to acids by NiO_2 nanoparticles (NPNPs) in water. Catalysts, 13(4): 645. https://doi.org/10.3390/catal13040645

[17] Li, S., Liu, A., Yang, Z., Zhao, L., Wang, J., Liu, F., You, R., et al. (2019). Design and preparation of the WO_3 hollow spheres@PANI conducting films for room temperature flexible NH_3 sensing device. Sensors and Actuators B: Chemical, 289: 252-259. https://doi.org/10.1016/j.snb.2019.03.073

[18] Jawaher, K.R., Indirajith, R., Krishnan, S., Robert, R., et al. (2018). A high sensitivity isopropanol vapor sensor based on Cr_2O_3–SnO_2 heterojunction nanocomposites via chemical precipitation route. Journal of Nanoscience and Nanotechnology, 18(8): 5454-5460. https://doi.org/10.1166/jnn.2018.15396

[19] Dubey, U., Maurya, A., Rawat, M., Tiwari, D., Chalotra, A. (2023). Synthesis of adsorbent from rubberwood sawdust (Hevea brasiliensis). Materials Today: Proceedings. https://doi.org/10.1016/j.matpr.2023.01.345

[20] Aziz, S.B., Marif, R.B., Brza, M.A., Hassan, A.N., Ahmad, H.A., Faidhalla, Y.A., Kadir, M.F.Z. (2019). Structural, thermal, morphological and optical properties of PEO filled with biosynthesized Ag nanoparticles: New insights to band gap study. Results in Physics, 13: 102220. https://doi.org/10.1016/j.rinp.2019.102220

[21] Thakur, A.K., Choudhary, R.B., Majumder, M., Majhi, M. (2018). Fairly improved pseudocapacitance of PTP/PANI/TiO2 nanohybrid composite electrode material for supercapacitor applications. Ionics, 24(1): 257-268. https://doi.org/10.1007/s11581-017-2183-x

[22] El-Naggar, A.M., Heiba, Z.K., Kamal, A.M., Mohamed, M.B., Altowairqi, Y. (2024). Tuning the structural, optical and dielectric features of PMMA/PEO/PANi blend using nano MnFe2O4. Optical Materials, 154: 115705

[23] Heeger, A.J. (2001). Semiconducting and metallic polymers: the fourth generation of polymeric materials. The Journal of physical chemistry B, 105(36): 8475-8491. https://doi.org/10.1021/jp011611w

[24] Hussain, F., Hojjati, M., Okamoto, M., Gorga, R.E. (2006). Review article: Polymer-matrix nanocomposites, processing, manufacturing, and application: An overview. Journal of Composite Materials, 40(17): 1511-1575.

[25] Bhadra, J., Alkareem, A., Al-Thani, N. (2020). A review of advances in the preparation and application of polyaniline based thermoset blends and composites. Journal of Polymer Research, 27(5): 122. https://doi.org/10.1007/s10965-020-02052-1

[26] Wen, J., Wang, S., Feng, J., Ma, J., et al. (2024). Recent progress in polyaniline-based chemiresistive flexible gas sensors: design, nanostructures, and composite materials. Journal of Materials Chemistry A, 12(11): 6190-6210. https://doi.org/10.1039/D3TA076

[27] Al-Saadi, A.A., Haroon, M., Popoola, S.A., Saleh, T.A. (2020). Sensitive SERS detection and characterization of procaine in aqueous media by reduced gold nanoparticles. Sensors and Actuators B: Chemical, 304: 127057. https://doi.org/10.1016/j.snb.2019.127057

[28] Zhu, G., Zhang, Q., Xie, G., et al. (2016). Gas sensors based on polyaniline/zinc oxide (PANI/ZnO) hybrid film for ammonia detection at room temperature. Chemical Physics Letters, 665: 195-199. https://doi.org/10.1016/j.cplett.2016.10.068

[29] Yamazoe, N., Shimanoe, K. (2008). Theory of power laws for semiconductor gas sensors. Sensors and Actuators B: Chemical, 128(2): 566-573. https://doi.org/10.1016/j.snb.2007.07.036

[30] Almaev, A.V., Kushnarev, B.O., Chernikov, E.V., Novikov, V.A., Korusenko, P.M., Nesov, S.N. (2021). Structural, electrical and gas-sensitive properties of Cr_2O_3 thin films. Superlattices and Microstructures, 151: 106835. https://doi.org/10.1016/j.spmi.2021.106835

[31] Blazinic, V., Ericsson, L.K., Muntean, S.A., Moons, E. (2018). Photo-degradation in air of spin-coated PC60BM and PC70BM films. Synthetic metals, 241: 26-30. https://doi.org/10.1016/j.synthmet.2018.03.021

[32] Wu, N., Guo, H., Peng, L.P.,Wnag, M.Y., et al. (2021).

A novel core-shell nanomaterial ratiometric fluorescent probe for detecting urinary TDGA as a biomarker for VCM exposure. Sensors and Actuators B: Chemical, 345: 130402. https://doi.org/10.1016/j.snb.2021.130402

[33] Konuk Ege, G., Akay, Ö., Yüce, H. (2023). A chemosensitive-based ammonia gas sensor with PANI/PEO–ZnO nanofiber composites sensing layer. Microelectronics International, 42(3-4): 29-35. https://doi.org/10.1108/MI-04-2023-0051

[34] Zhou, P., Tsang, J.H., Blackman, C., Shen, Y., et al. (2024). A novel mechanism based on oxygen vacancies to describe isobutylene and ammonia sensing of p-Type Cr_2O_3 and Ti-doped Cr_2O_3 thin films. Chemosensors, 12(10): 218. https://doi.org/10.3390/chemosensors12100218